Energy Conversion and Management: X 24 (2024) 100789

Contents lists available at ScienceDirect

Energy Conversion and Management: X

journal homepage: www.sciencedirect.com/journal/energy-conversion-and-management-x

Optimal design of a series hybrid powertrain for an agricultural tractor

Manuel Antonio Perez Estevez [a], Joaquim Melendez Frigola [b], Joaquim Armengol Llobet [b], Luigi Alberti [c], Massimiliano Renzi [d,*]

[a] Scuola Universitaria Professionale della Svizzera Italiana, Via Flora Ruchat-Roncati 15, Mendrisio, 6850, Ticino, Switzerland
[b] Universitat de Girona- Escola Politècnica superior, C/Ma Aurèlia Capmany, 61, Girona, 17003, Girona, Spain
[c] Università di Padova, Via VIII Febbraio, 2, Padova, 35122, Padova, Italy
[d] Free University of Bozen-Bolzano, Piazza Università, 1, Bolzano, 39100, Bolzano, Italy

ARTICLE INFO

Keywords:
Tractors
Powertrain architecture
Powertrain optimization
Emissions reduction
Series hybrid

ABSTRACT

Hybrid powertrains represent a potential solution to reduce the emissions of agricultural machineries and meet the restrictive standards introduced by the different governments with the aim to achieve Climate Neutrality. This study investigates a hybrid powertrain in the series architecture as it potentially better suits the requirements of agricultural applications, even though it has not yet been fully investigated in literature. A series hybrid powertrain model was built, then its control and components size were optimized for a vineyard/orchard tractor using real on-field data and a two level optimization procedure. This last is based on Dynamic Programming and the exhaustive search approach. Both environmental and economical aspects were taken into account in the optimization goals; in addition, powertrain volume constraints were introduced as they represent a key limiting factor for tractor hybridization. The average efficiency of the hybrid powertrain is higher than that of the conventional configuration. A sensitivity analysis was performed to understand the impact of different design parameters. This analysis showed that hybrid powertrains have enormous potential in the agricultural market, as this type of configuration was simulated in several scenarios for different European countries showing to be the most convenient. Moreover, this trend is expected to intensify with the upcoming emissions regulations and the increase in fuel prices through emission taxes.

1. Introduction

Since the mid 1990s, increasing attention is being paid to off-road vehicles emissions, where tractors are one of the most impacting. Tractors' NOx emissions and Particulate Matter (PM) are the most critical because of their nocivity and the great fraction over the total produced by this type of machines [1]. Anyway, the reduction of their greenhouse emissions plays an important role to achieve Climate Neutrality, which was set as EU objective for 2050, and also the target of limiting global warming to 1.5 °C by the end of this century as stated in the Paris Agreement [2]. This is specially true in a market where the number of tractors is increasing. In order to reduce emissions, worldwide authorities have implemented new standards that force the agricultural machinery manufacturers to produce new machines that comply with certain technical provisions. The predominant solutions applied so far are based on Internal Combustion Engines (ICEs), as they fit the existing powertrain structure; these solutions include: Selective Catalytic Reduction (SCR), Exhaust Gas Recirculation, Diesel Oxidation catalyst and Diesel Particulate filters [3]. Anyway, the technological problem persists in many cases since adding new pollution control devices is expensive and necessitates more volume and space is a valuable resource that can have a significant impact on tractors structure [3,4]. Moreover, the increase of tractors nominal power and their number overcome the benefits of these solutions, which combined with the requirement of more restrictive limitations in the future introduces the necessity for new technical solutions [1,3].

Electrified powertrains is the most adopted solution in on-road vehicles to overcome these problems. The potential of electric and hybrid powertrains have been demonstrated in several scientific publications and practical cases [5–7]. Therefore, the interest of this type of powertrain in the off-road machinery industry has increased. Still, the diverse and more demanding working conditions of tractors make their implementation quite challenging; tractors do not just need to propel themselves, but also provide power to different implements and pull different loads. The main obstacles highlighted until now are: (i) the fact that tractors are usually required to work for 8 continuous hours, (ii) the required power density and (iii) the high price of batteries. The first step to promote electrified tractors and obtain satisfactory

* Corresponding author.
E-mail address: massimiliano.renzi@unibz.it (M. Renzi).

https://doi.org/10.1016/j.ecmx.2024.100789
Received 17 September 2024; Received in revised form 4 November 2024; Accepted 5 November 2024
Available online 19 November 2024

Nomenclature

c	battery C-rate (power based)	T_r	torque ratio
c_{EE}	cost of the electric energy from the grid	V	volume of powertrain component
c_{fuel}	agro-diesel cost	$V_{allowed}$	volume allowed
$Cost$	powertrain component cost	WC	white certificates costs
E_{bat}	battery energy capacity	x	scaling factor
f	fuel consumption	α	grid emission factor
$\dot{f}$	fuel flow	β_1	drivability coefficient 1
$\dot{f}_s$	fuel flow — static condition	β_2	drivability coefficient 2
HV	heating value	η_{bat}	battery efficiency
J_{global}	global cost function	$\eta_{charge-grid}$	efficiency of charging from the grid
$J_{control}$	cost function related to powertrain control	η_{EM}	EM efficiency
$J_{components}$	cost function related to components sizing	η_{ICE}	ICE efficiency
n_d	speed @ engine rated power	η_o	ICE nominal efficiency
n_{d-ref}	reference ICE nominal speed	η_{PW-e}	average efficiency — electric powertrain
n_i	instantaneous speed	η_{PW-t}	average efficiency — traditional powertrain
P_{base}	nominal power of the reference component		
P_{chem}	battery power considering its efficiency	μ_n	speed coefficient of performance
P_e	max. ICE power @ instantaneous velocity	μ_p	power coefficient of performance
$P_{EM-d-ref}$	reference EM nominal power	ω_{base}	nominal speed of the reference component
P_{ICE}	instantaneous ICE power	$\omega_{EM-d-ref}$	nominal speed of the reference EM
$P_{ICE-d-ref}$	reference ICE nominal power	ω_r	speed ratio
P_{scaled}	nominal power of the target component	$omega_{scaled}$	nominal speed of the target component
R	transmission ratio	ρ	diesel density
SOC	State of Charge	τ_{base}	nominal torque of the reference component
SOC_o	initial SOC	$\tau_{EM-d-ref}$	nominal torque of the reference EM
T_{max}	electric motor max. torque ratio curve	τ_{scaled}	nominal torque of the target component

performance is their correct design. In case of hybrid powertrains, the design cannot be isolated from the control of the powertrain [8–10]. In literature some studies about electric and hybrid tractors are available; the majority has been produced in recent years. Brenna et al. [11] sized the main components for a 157 kW electric tractor based on two working conditions: the maximum towable mass and soil tillage during a whole day of work. They found that the capacity of the battery required is 662.2 kWh and that, even if the battery cost increases the initial investment, the use of an electric tractor will bring economical benefits when the operational and maintenance cost are considered. Similarly, in [12] the powertrain of a small electric tractor (18 kW) with a dual motor configuration was designed. A battery capacity of 38.9 kWh was obtained in this work. These studies did not consider the fact that many farmers are not willing to pay such a high investment cost and that in most of the cases the space available in tractors is not enough to carry a battery able to last 8 h when working at typical operating conditions [13]; reduced duration means reduced productivity. The space consideration is specially critical for narrow tractors used in vineyard and orchards. In fact, the implementation of Stage V of the European Emissions Standards for tractors with powers between 56 kW and 130 kW has been delayed with respect to the other powers, since small-sized ICEs with the solutions mentioned above are incompatible with the space requirements of these tractors [14,15].

Hybrid powertrains could overcome electric tractors limitations highlighted above due to the use of a smaller battery, but still provide consistent environmental benefits. Another possible solution that is being studied to overcome these problems is the usage of electric autonomous tractors, where the cabin space is used to place a bigger battery. The authors of [16] found that in a simulated scenario an electric autonomous tractor has comparable prices to traditional tractors, but it presents a significant delay in terms of operation. Companies are also working in this direction; John Deere is an example of this [17] and their *Sesam* project is a clear demonstration [18]. Anyway, this type of solution is not the focus of this work and, thus, it will not be further discussed here. Moreover, the authors believe that hybrid powertrains will represent a preliminary step of tractors industry towards environmental friendly solutions. In [19] was studied the potential of a parallel hybrid configuration for a 66 kW tractor. The simulations carried out suggest an improvement of fuel economy of 19.2% compared to the traditional configuration. Similarly, Dalboni et al. [20] proposed the downsizing of the ICE of a traditional tractor from 77 kW to 55 kW using a hybrid parallel configuration. The new power was selected to make the new ICE belong to a different category with less restrictive conditions according to the European Stage V Non-Road Emission Standards [21]. The simulation results presented show that the hybrid configuration bring benefits in terms of fuel consumption for all the duty cycles studied. Moreover, the authors mentioned that this solution needs limited effort to convert an existing machine; in fact, a prototype was already under construction using a preexisting platform. The battery capacity selected (25 kWh) was the highest that fits the engine compartment of the tractor, which confirms that volume plays a key role in tractors electrification. Economical aspects were not considered in these studies, which are critical to assess the feasibility of use of a certain technology. On the other hand, Beligoj et al. [22] proposed a method based on life cycle cost to downsize the ICE of a tractor using a parallel hybrid configuration. Different tractor sizes were studied, obtaining that cost savings increased for small tractors. One of the objectives considered in this work was to keep battery capacity as small as possible to meet the technical requirements of realistic encumbrance, but ignoring the fact that bigger batteries could bring to bigger environmental benefits. Other studies about parallel hybrid tractors design, control and performance could be found in the literature [23,24]. Studies that focus on control are crucial to improve the performance of existing vehicles, but hybrid tractors development is still a step backwards. Anyway, as was already mentioned, design is tied to control and, to the knowledge of the authors of the present work, none of these studies deal simultaneously with design and control, as it has already been done for other vehicles [8,25,26].

Few studies about tractors with a series hybrid configuration are available in the literature. In [27], the possibilities of the use of a series hybrid tractor, where the typical diesel ICE was substituted by a Compressed Natural Gas (CNG) engine, is investigated. The authors

Table 1
Hybrid powertrain tractor's studies available on the literature.

Architecture	Study type	Year range	Quantity	References
Full Electric	–	2018–2019	2	[11,12]
Parallel	Design and Performance	2013–2022	10	[19,20,24,35–37] [15,22,38,39]
Parallel	Control	2013–2020	2	[23,40]
Series	Design and Performance	2022	2	[15,27]
Series	Control	2014–2021	4	[28,29,41,42]
Others	–	2019–2022	3	[37,43,44]

conclude the convenience of this type of technology depends on the powertrain management. In any case, the authors did not discuss tractor autonomy in detail, which could be a critical aspect considering CNG storage volumes. Jia et al. [28] studied two rule-based power management strategies on a series hybrid tractor. The same authors further worked on energy management strategies demonstrating that approaches based on optimal control could get improvements in fuel efficiency of up to 5% compared to the typical rule based management [29]. More complex architectures have also been investigated in the literature, but the requirement of more components increases complexity and goes against the space limitations. Table 1 reports some of the studies about hybrid tractors available in the literature; an important fact that should be highlighted, is that almost none of these studies deal with optimal design. Furthermore, it can be seen that parallel hybrid dominates the academia interest, which is different to what is happening at an industrial level where electric and series hybrid tractors have received more attention (see Table 2). Kubota, Monarch and Fendt are developing electric tractors that would be commercialized in the coming years [30–32]. Moreover, Solectrac, an American company, already introduced two electric tractors to the market [33]. All these tractors have limited autonomy, less than 8 h. In order to overcome this problem, Monarch and Solectrac offer the possibility of having exchangeable batteries, but this would require the acquisition of more than one battery which is an expensive component. John Deere is also studying different technologies to get over this limitation; one of them is "GridCON2" the latest version of a cable connected electric tractor [34].

Diesel–electric tractor is a solution that has already been implemented at a commercial stage to reduce emissions, it consists of an ICE-Generator pair connected to an Electric Motor (EM) responsible to transmit the power to the wheels or implements. This solution is similar to a series configuration but without battery, therefore the only possibility of improvement is due to the elimination of the dependency of the ICE working point from the load. Steyr Konzept, a series hybrid tractor prototype, was presented at Agrotechnica 2019. CNH Industrial America LLC claims that Steyr Konzept is able to reduce fuel consumption of about 8%, without limitations in autonomy [45]. On 2021, Carraro Spa brought for the first time the idea of a parallel tractor configuration for a vineyard/orchard tractor [46]. Other off-road vehicles as wheel loaders [47,48], excavators [49] and tower yarders [50,51] have been proposed with a series configuration, which could suggest that also the tractor's market will follow this trend. Table 2 summarizes some of the industry more important prototypes and commercialized electrified tractors.

Furthermore, the works [15,52,53] were the only ones to the authors' knowledge where different hybrid configurations for tractors are compared. In [15], the series configurations had the highest fuel savings, despite the need of double energy conversion. In parallel configurations, the engine was forced to work at low efficiency points most of the time due to the direct connection of the load and the ICE. Similarly, the authors of [52,53], modeled different powertrain setups using a similar approach based on "Autonomie" simulation software. Both studies indicate that hybrid configurations can enhance fuel efficiency and reduce emissions compared to the traditional configuration. However, the first study suggests that parallel configurations might offer higher efficiency, while the second supports the findings of [15] that series configurations consume less fuel. These discrepancies may stem from the different reference working loads used; the first study focused on a tractor performing tilling operations, while the second used a custom-defined cycle simulating straw wrapping and baling. It is to be highlighted that none of these studies optimized the powertrain configurations; they only conducted simulations based on existing models, making it difficult to effectively determining the most efficient architecture. Additionally, space constraints necessary for achieving technically feasible configurations were only briefly mentioned in [52]. Overall, the results from these three papers collectively support the market trend of adopting series hybrid powertrains for these applications. For off-road mobile machinery, the most important advantages of a series hybrid powertrain are: (i) architecture with a lower complexity level: no need of complex transmission systems, which could translate into lower maintenance costs and, therefore less downtime; (ii) the ICE could work most of the time at high efficiency points, since it does not directly power the vehicle or the Power Take-Off (PTO); (iii) silent and with less vibrations; and (iv) less harmful as the ICE could work at a point with low pollutant emissions or at pure electric mode when operators are around the machine. The last point is also important since tractors are surrounded by crops.

Based on all that has been discussed previously, the aim of this work is to fill the gap of the design of series hybrid powertrains for tractors; which, as has been shown above, are more aligned with the industry interests. Matching the industry interests is important to contribute and accelerate the deployment of this technology and, therefore, the reduction of the emissions of the agricultural sector. The optimization procedure used in this work considers not just the powertrain design but also its control. To the knowledge of the authors this simultaneous approach, which could get better results than the one considering only the design, has not yet been introduced to tractors powertrain design. The above mentioned procedure utilizes a Dynamic Programming (DP) algorithm combined with exhaustive search and has been applied to an orchard/vineyard tractor using real load data. In order to obtain solutions that help reducing emissions, but are still commercially feasible, the objective function considers both the economical and environmental aspects. Notably, the optimization also considers the volume available for the powertrain — a critical factor often overlooked in existing literature. This constraint is essential because the physical dimensions of a tractor significantly impact its design and functionality. By factoring in volume limitations, the optimization ensures that proposed powertrain solutions are practical for integration into existing tractor architectures, making the outcomes not only efficient but also feasible for manufacturers to implement.

Global markets, particularly in fuel and energy, are currently experiencing high volatility. In many European countries, the price of agricultural diesel has risen significantly — due in part to new policies and political situations — leading to increased operational costs for diesel tractors. A key innovative aspect of this work is the investigation of the most suitable powertrain architecture — whether traditional, hybrid, or electric — under varying boundary conditions and design parameters, especially when these factors change simultaneously. This enables a thorough sensitivity analysis to identify the most advantageous architecture for different scenarios across European countries and also future scenarios. This approach, and also in particular this study, can assist manufacturers and policymakers in making informed

Table 2
Electrified tractors and prototypes — Industry.

Company	Model	Architecture	Year	Power [kW]
John Deere	7530 E-Premium	Micro hybrid (aux. electrified)	2009	156
Belarus	3023	Diesel–electric (series no battery)	2009	220
CNH-New Holland	NH2	Fuel Cell	2011	100
Fendt	e100 Vario	Electric	2018	70
Fendt	X concept series	Diesel–electric (series-no battery)	2019	147
Argo Tractors — Landini	REX4 Electra	Series–parallel	2021	80
CNH-Steyr	Konzept	Series	2019	250
Monarch	MK-V	Electric	UD[a]	30
Auga	M1	Series (biomethane–electric)	UD[a]	300
Antonio Carraro	SRX hybrid	Parallel	2021	75
Solectrac	e25	Electric		19
Solectrac	e70	Electric		52
Kubota	LXe-261	Electric	2023	19

[a] UD = Under Development.

Table 3
Target powertrain characteristics.

ICE nominal power [kW]	80
ICE volume [m^3]	0.25
Transmission volume [m^3]	0.1
Rear wheel radius [m]	0.7

decisions by identifying configurations that are technically feasible and in line with industry requirements.

The rest of the paper is organized as follows: Section 2 reports the data of the target tractor and working cycles; Section 3 describes this work methodology, specifically, the model and the optimization procedure; the results of this work together with their analysis are reported in Section 4 and finally Section 5 provides the most important highlights of this work and some suggestions for future work.

2. Target tractor and working cycles data

This study focuses on two vineyard/orchard tractors with similar characteristics; in particular, the data of the tractors studied in [24,39] have been used as reference to define the working conditions for a period of 8 h. In Table 3 are reported the details of the target powertrain, the volume of the components was determined by averaging the one of tractors with a nominal power in the same range than the target one.

Standardized working cycles are not well defined for the study of hybrid powertrains for non-road mobile machinery. Testing under the Non-road Transient Cycle (NRTC) [54] is the procedure required by different standards (EU Stage V, US EPA Tier 4 and Japanese 2011/13 regulations) to certify the ICE. Unlike road vehicles, where cycles give a time–velocity profile that then determines the load depending on the vehicle, NRTC is based on the characteristics of the currently installed ICE and the working cycle is defined through the use of its normalized speed and torque. Furthermore, in most cases this cycle does not describe a condition similar to an actual use. This, together with the limited information available about tractors daily working conditions, makes designing electrified powertrains for tractors very challenging. In fact, many studies are based solely on critical working conditions. Conversely, this work is based on actual field measurements from [24,39] and, therefore, it grants a higher reliability of the results. The power, torque and speed required by the major loads of the tractor, which are the traction system, the PTO and the oil pumps for the hydraulic devices, were identified. Specifically, six working cycles were used as reference, Table 4 reports a general description of them, while Fig. 1 reports the power profiles for the atomizer and tying operations. The transport working cycle consists only of an acceleration test until the maximum tractor speed (without tow). No further details of the measurements are reported for conciseness and due to confidentiality reasons.

Combining the previous cycles, a work cycle with a duration of 8 h was created, which is the duration of a typical working day in the agricultural field. Although, a scenario where all these operations consecutively occur is not realistic, a single cycle was built to make the optimization procedure find a solution (powertrain) capable of performing all the operations but still maximizing the efficiency in each of them. The power profile was divided into three parts: Light-medium duty, Heavy duty and Rest with a respective duration of 3.37, 4.20 and 0.35 h. The exact length of the cycle was 7.92 h; it could be considered that the missing time, to complete the 8 h, the tractor was at rest at the beginning of the working day. The heavy duty component was placed at the end of the cycle to ensure that the tractor is capable of the more power demanding tasks in the second half of the day. The authors expect the battery State of Charge (SOC) to be low after probably been used for the Light-medium duty component. The order of the cycles in each part was set by a random function; however, blocks of the same cycle in the Heavy duty component were set together to resemble as close as possible the actual working conditions. The exact composition of the daily cycle is reported below:

1. Light-medium duty: Grape Harvesting, Transport, Tying and Plant lifting plough;
2. Heavy duty: 4 Atomizer cycles + 2 Weeder cycles;
3. Rest: two minutes of rest, without power requirement, after each task and 20 s at the beginning of the profile.

The theoretical total fuel consumption of the daily cycle with a traditional powertrain was estimated to be 58.31 L and it was calculated by summing up the consumption of the different tasks. It should be highlighted that the order of the profiles may slightly change the optimization results.

3. Methodology

In this section the system model and the optimization procedure are described.

3.1. Powertrain model

3.1.1. Preliminary analysis — Electric powertrain

In this section, an electric tractor capable of performing the above 8-hours cycle is designed. Fuel consumption has been translated to energy requirements by means of Eq. (1) and the data reported in Table 5. The electric energy and battery capacity needed were estimated to be 172.1 kWh and 215 kWh, respectively. The battery capacity considers a safety margin of 20% to avoid fully discharging the battery, and to consider aging and more demanding cycles. Nowadays, lithium-ion batteries have an energy density of about 240 Wh/l [55,56], this means the volume of the battery needed will be of 0.9 m^3 which is more than double of the volume currently occupied by the main components of

Table 4
Working cycle characteristics.

Operation	Class	Time [s]	Avg. power traction[a]	Avg. power PTO[a]	Max. power system[a]	Avg. speed km/h	Fuel consumption [l]
Atomizer	Heavy	1593	9	24	50	7	5.06
Weeder	Heavy	4370	26	0	63	5	12.00
G. Harvester	Med.	4359	2	10	37	2	7.63
Transport	Light	152	9	0	67	18	0.23
Lifting plough	Light	4303	3	0	28	4	4.49
Tying	Light	3317	−0.1	0	5	1	1.72

[a] Power in kW.

Table 5
Fuel characteristics and powertrains efficiencies.

Variable	Symbol	Value
Fuel consumption [l]	f	58.31
Diesel density [kg/l]	ρ	0.85
Heating value [MJ/kg]	HV	44
Average efficiency traditional powertrain [–]	η_{PW-t}	0.25
Average efficiency electric powertrain [–]	η_{PW-e}	0.88

Diesel properties has been taken from [57].

the traditional powertrain (see Table 3). Based on this result, it could be said that, in order to be technically feasible, fully electric tractors require further improvements of battery density and/or the complete rearrangement of the tractor architecture. Thus this study focus on hybrid tractors, specifically on a series configuration.

$$E_{electric} = \frac{f \cdot \rho \cdot HV \cdot \eta_{PW-t}}{3.6 \cdot 10^6 \cdot \eta_{PW-e}} \quad (1)$$

3.1.2. Series powertrain

The architecture of the series hybrid powertrain adopted in this work is presented in Fig. 2. Although, electric motors are known for their flexibility and high efficiency when working in off-design conditions (loads and speeds) when compared to ICEs, it was necessary to use a two gears transmission system to make the system capable of performing all the tasks. Conventional tractors powered with an ICE include a complex and cumbersome transmission, with up to 64 combinations, to meet all the possible torque and speed demands [58]. In fact, tractors work at high speeds during transportation, almost zero speed during tying and at high torques and constant mid speed during atomizing. This last condition could be very detrimental to the environment due to the connection between the PTO and the traction system, as ICEs are highly sensitive to the operating conditions in terms of efficiency and emissions. One possibility to overcome this problem is powering the PTO with a stand-alone electric motor, solution that has already been adopted by some manufacturers. This approach decouples the rotational speed of the ICE from that of the PTO. As it is shown in the results of the paper, the volume of the powertrain revealed to be a critical factor in terms of design of the electrified tractor; therefore, thanks to the high electric motors efficiency at almost all the working conditions, the same motor used to power the traction system is also used to run the PTO. On the other hand, it was decided to electrify the hydraulic system using electro-pumps connected to the battery through a DC–DC converter that adapts the battery voltage to the one of the actuator; this avoids the use of further gears to connect the pumps to the main shaft — mechanical connection (see Fig. 2).

The description of the models used to simulate the behavior of the different components of the powertrain reported in Fig. 2 is presented hereinafter.

ICE: it was modeled according to [59], because of the flexibility of this approach to simulate engines of different sizes by just changing few input data. This model calculates the ICE efficiency using two single dimension polynomials that decouple the speed and power influence. Moreover, the authors of [59] validated their model using data of different vehicles (type and size). The engine efficiency (η_{ICE}) and the fuel consumption rate ($\dot{f}$) can be calculated using the following equations:

$$\eta_{ICE} = \eta_o \mu_p \mu_n \quad (2)$$

$$\mu_p = 0.60 - 0.17\frac{P_{ICE}}{P_e} + 2.50\left(\frac{P_{ICE}}{P_e}\right)^2 - 2.11\left(\frac{P_{ICE}}{P_e}\right)^3 \quad (3)$$

$$\mu_n = 0.711 + 0.996\frac{n_i}{n_d} - 1.058\left(\frac{n_i}{n_d}\right)^2 + 0.312\left(\frac{n_i}{n_d}\right)^3 \quad (4)$$

$$\dot{f}_s = \frac{P_{ICE}}{\eta_{ICE}\rho HV} \quad (5)$$

$$\dot{f} = \dot{f}_s + 0.2\dot{f}_s\left|\frac{P_{ICE-p} - P_{ICE}}{P_{ICE-d}}\right| \quad (6)$$

where η_o is the engine nominal efficiency, P_{ICE} and n_i are the ICE instantaneous power and speed, respectively, n_d is the speed corresponding to the engine rated power, P_e is the maximum engine power at the corresponding instantaneous velocity, the subscripts p and d in Eq. (6) refer to the power in the previous step and the ICE rated power, respectively, and lastly, the subscript s refers to the static fuel consumption. The second term of Eq. (6) was added by the authors of this study to include the additional fuel consumption of the engine due to its transients [60–62]; in [61,62] were reported increases of up to 14% and 100%, respectively. The maximum power curve of the engine was modeled using Eq. (7), which was obtained by fitting the power curve of a **DEUTZ TCD 2.9 L4** engine for agricultural purposes. The nominal power of this engine is 55.4 kW, which is consistent with the expected ICE size of the optimization procedure. The fuel consumed in one cycle can be calculated as the integral of the fuel consumption rate.

$$P_e = P_{ICE-d}\left(9.5\frac{n_i}{n_e}^4 - 28.2\frac{n_i}{n_e}^3 + 28.7\frac{n_i}{n_e}^2 - 10.7\frac{n_i}{n_e} + 1.7\right) \quad (7)$$

Electric motor and generator: the efficiency map of the motor presented in [63] was normalized using the maximum motor speed and torque. Once a dimensionless map was obtained, it was fitted using as input variables the ratios of torque (T_r) and speed (w_r). Eq. (8) shows the result. A similar approach was used to obtain the maximum torque curve (T_{max}), which is reported in Eq. (9). The efficiency map taken as reference already considered the inverter efficiency.

$$\eta_{EM} = 0.80 + 0.18w_r + 0.31T_r - 0.12w_r^2 + 0.84w_rT_r - 0.90T_r^2 - 0.66w_r^2T_r - 0.18w_rT_r^2 + 0.54T_r^3 \quad (8)$$

$$T_{max} = \begin{cases} 1 & \text{if } w_r <= 0.3 \\ -2.25w_r^3 + 5.59w_r^2 - 4.96w_r + 1.90 & \text{if } w_r > 0.3 \end{cases} \quad (9)$$

The efficiency of the operating conditions characterized by a negative torque value, thus those corresponding to the generator, was determined by replicating the curves shown earlier, but this time utilizing the absolute value of the torque ratio.

Battery: the SOC change of the battery was modeled using Eq. (10), which is an energy counting approach. Then, the SOC was calculated

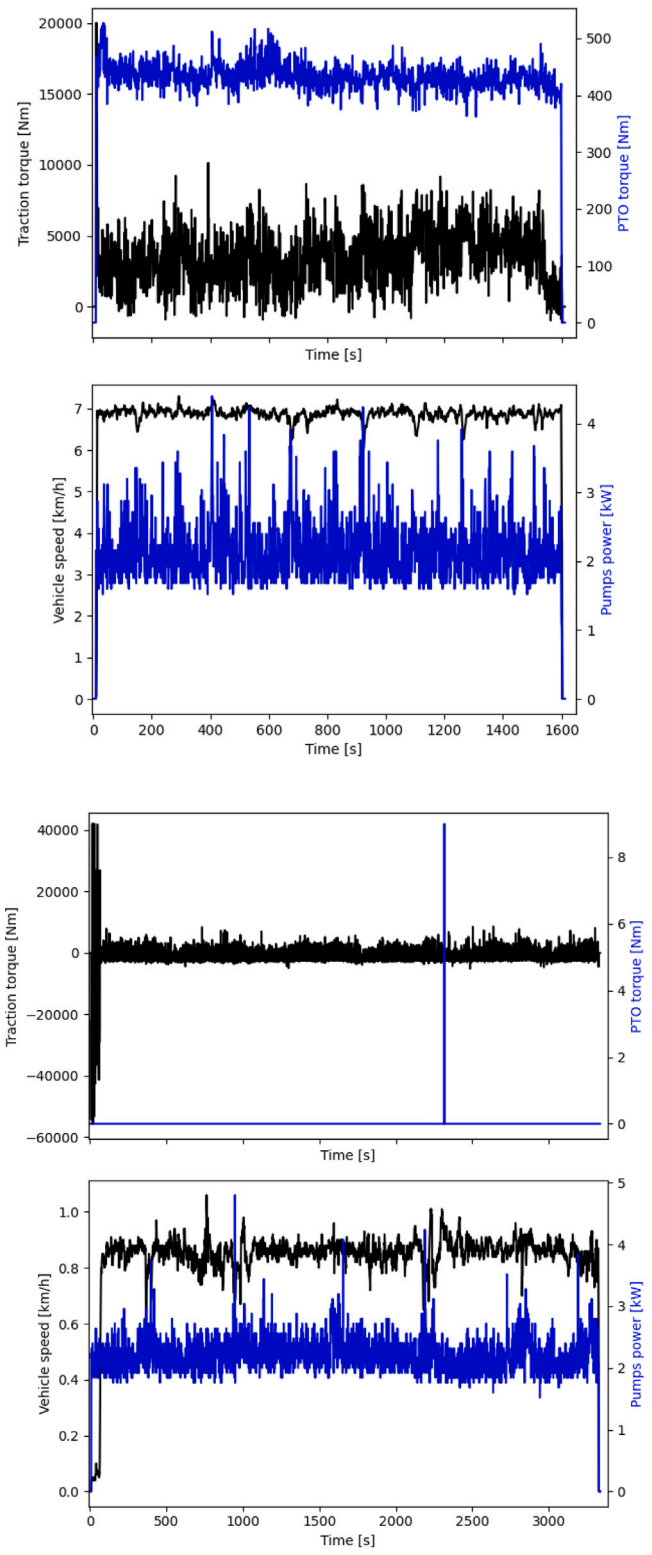

Fig. 1. Load curves: top — atomizer and bottom — tying operation.

integrating this equation, which was done using a fourth order Runge Kutta function. The above mentioned approach was preferred with respect to the typical Coulomb counting method because this last needs the previous definition of a battery configuration in order to fix the battery pack voltage. In this case, the battery detailed configuration is not needed since it is a first estimate-convenience analysis, which suits more general models with less assumptions.

$$\frac{dSOC}{dt} = -\frac{P_{chem}}{3.6{\cdot}10^6 E_{bat}} \tag{10}$$

where E_{bat} is the battery capacity in terms of energy and P_{chem} is the instantaneous power of the battery considering the battery efficiency, which was estimated using Eq. (11), reported in [64]. The battery maximum power was set to 2C and 5C for charging and discharging conditions, respectively.

$$\eta_{bat} = \begin{cases} 0.002232 \cdot c^2 - 0.0246 \cdot c + 1 & \text{discharging} \\ 0.0033 \cdot c^2 - 0.0297 \cdot c + 0.99814 & \text{charging} \end{cases} \tag{11}$$

where c corresponds to the battery C-rate in terms of power; thus, the battery power divided by the battery energy capacity.

Mechanical transmission systems: the mechanical conversion devices were modeled using Eqs. (12) and (13). The first equation was related to the rotational speed ω, while the second to the torque τ. The gearbox and speed reducer were considered using a ratio (R) that includes both and in this case the efficiency was set to 0.95. On the other hand, the efficiency of the single gear between the ICE and generator and the PTO gear was considered of 0.98.

$$\omega_{out} = \omega_{in} \cdot R \tag{12}$$

$$\tau_{out} = \tau_{in}/R \cdot \eta_{transmission} \tag{13}$$

Control: in this study four control possibilities were considered for the powertrain:

- Control 1: all the power is provided by the battery. The ICE-GEN (GENSET) block is disconnected and turned off by means of an electrical switch placed between the rectifier and the inverter. This mode is not preferred when the battery SOC is below 0.5 to avoid the powertrain is unable to perform other more demanding tasks in the remaining working hours of the day. In a real implementation, this limit could be deactivated in the control system, but in this work it was always considered.
- Control 2: the engine works at its maximum efficiency point. In case of power surplus it is used to charge the battery, while in case of more power required by the loads this is provided by the battery.
- Control 3: the engine works at is maximum power point. The battery behaves in the same way as for Control 2.
- Control 4: all the power is provided by the ICE, included the power of the pumps, which should go through the electric components of the powertrain. In this condition the engine speed is fixed to the one of the maximum efficiency point; in case of the reference engine taken in this study this is equal to 70% of the maximum one. The only exception is when the power demand is equal or below to zero, in this case the ICE works in idling condition. This control method could only be adopted when the required power is below than the maximum power of the ICE considering the corresponding efficiencies.

Within this approach, additional working points, as for example, a point to minimize the nitrogen oxides or other harmful emissions could be added to the powertrain controller; this could help to meet specific emissions regulations or objectives.

It was set that the battery can recover energy only when its SOC is less than 0.85, in other cases it is dissipated by the brakes. That is, if the load is negative but the SOC is higher than 0.85, then this power cannot be used to charge the battery and is dissipated by the brakes. This was assumed to avoid excessive battery aging, due to uncontrolled charging currents. In addition, in all cases the battery power limits are considered, this has been done by adding constraints and penalties and it will be explained in detail in the next section.

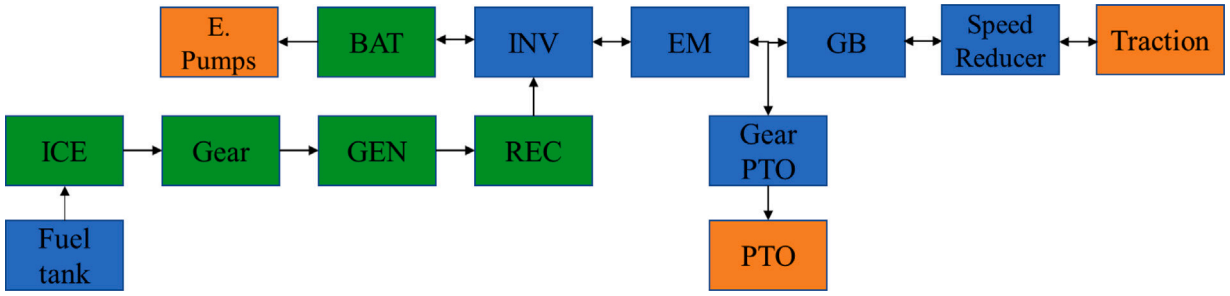

Fig. 2. Series powertrain configuration scheme. BAT: battery; INV: inverter; EM: Electric motor; GB: gearbox; ICE: internal combustion engine; GEN: generator and REC: converter–rectifier. Colors — Orange: loads; Blue: design previous to optimization; Green: optimized design. (For interpretation of the references to color in this figure legend, the reader is referred to the web version of this article.)

3.2. Optimization procedure

The optimization procedure was structured into two loops: an internal loop for powertrain control and an external loop for component sizing. This setup enables the identification of the optimal control strategy for each viable powertrain configuration, allowing a comparison to determine the global optimum. The optimum configuration is defined as the one that minimizes the value of Eq. (14), where the first term represents the control contribution and the second term reflects the component size. Notably, the control term intrinsically depends on the component sizing. The outer loop relies on an exhaustive search approach, building a model for each feasible configuration considering the input size possibilities specified by the user; Section 3.2.2 provides a more detailed explanation. Meanwhile, the internal loop utilizes dynamic programming (DP) to control the models generated by the external loop, finding the optimal control strategy for each, further details are given in Section 3.2.1.

The operational hours per year and the years of service of a tractor strongly vary depending on the owner and uses; farmers typically give less intensive use than agricultural contractors [65]. In this work, it was assumed that the tractor under study will work 100 days per year for 14 years; this means a lifespan of 11200 h, which is in the range suggested in [65] (10000–12000 h). The same cycle is repeated each day of work.

$$\min_{size-components,u} J_{global} = \min_{size-components,u} J_{control} \cdot days \cdot years + J_{components} \quad (14)$$

where J is the cost function, u is the vector of control actions and $size-components$ is the vector of sizes of each component that must be optimized.

3.2.1. Control

The optimal control solutions were found using DP, which is a method to solve optimization problems by breaking them into smaller subproblems and recursively finding the optimal solutions to each subproblem. DP is a well known algorithm that has been used to solve many optimization problems because of its capability to find the global optimum in a specific domain, thus several times taken as reference case. One limitation of this algorithm is that its computational demand and time grow with the number of states and variables, but in this design study this was not a restrictive issue. Further details of this algorithm could be found in [66,67].

In order to apply DP, the control problem of this study was discretized into intervals of one second; therefore, the best control action u could be found for each second, this action was considered constant during each time step. In this case, the optimization problem has two control actions: (i) u_1 **— the status of the powertrain** (four possibilities available, see section 3.1.2- Control) and (ii) u_2 **— the selected gear on the transmission system (GB)**, while it has one state variable: the SOC. The control actions were already discrete, so they did not require any additional procedure. On the other hand, the SOC is a continuous variable that needed to be discretized; in this case, 0.05 intervals were adopted, except for the first interval, which was from 1 to 0.9. At each time step the algorithm memorizes only the best possibility for every SOC range considering all the initial conditions. The latter are given by the final conditions of the previous step. For example: let us suppose that at time step #n two of the SOC initial conditions are 0.801 and 0.78, which belong to different SOC ranges. Suppose also that when the algorithm applies Control 1 to the first initial condition (0.801), the final SOC is lower than 0.8 and thus, it is in the next range of SOC, the system will compare it with all the possibilities of when the initial SOC was 0.78 and select the one with the lowest cost function, this assuming that after applying all the controls options to the second initial condition all the final SOCs stay in the range between 0.8 and 0.75.

A fitter grid for the SOC, for example of 0.01, gave better results in terms of control-related cost function, but this improvement was so small that it would have not changed the main conclusions of this work. Moreover, the additional computational time will have made the sensitivity analysis difficult and cumbersome.

Eq. (15) presents the control related cost function ($J_{control}$) to be minimized in this study; no terminal cost has been considered since the SOC was directly contemplated in the cost-function in order to allow the last time step to have a free value of the SOC (unknown at the beginning). The solution to this problem obeys the fundamental equation of DP: the value function at state k under the optimal policy is equal to the minimum of the sum of the transition cost from the previous stage and the value function of the preceding state under the optimal policy; thus, Eq. (16) was obtained. These equations consider economical and environmental aspects; in order to do this, all the emissions were converted into an economic cost. In particular, the first term considers the fuel contribution. The amount of fuel was transformed into an economic cost by multiplying it by its unitary price, which is supposed to include a component due to taxes for the emissions produced. The second term is related to the energy taken from the grid, the first part considers the economics, while the second considers how is the energy produced; therefore, the related emissions and their transformation to money through the use of white certificates. The terms accompanied by a β coefficient help to identify feasible solutions in terms of drivability, i.e., to avoid having the system change control every second even though this could provide a better cost function result; shifting gear and powertrain status could impact driver and passenger comfort, as well as the reliability of the mechanical and electrical components. On the other hand, P refers to all the penalties added to the system to obtain constrained and feasible solutions.

$$J_{control} = \sum_{t_o}^{t_f} (\dot{f} \cdot c_{fuel} + \Delta SOC \frac{E_{bat}}{\eta_{charge}} (c_{EE} + \alpha \cdot WC) + \beta \cdot \Delta u^2 + P) \cdot \Delta t \quad (15)$$

$$J_{control\,k}{}^*(x_{k+1}) = \min_{u_k} [(\dot{f} \cdot c_{fuel} + \Delta SOC \frac{E_{bat}}{\eta_{charge-grid}} (c_{EE} + \alpha WC) + \beta_1 \Delta u_1{}^2 + \beta_2 \Delta u_2{}^2 + P) + J_{control\,k-1}{}^*(x_k)] \quad (16)$$

where c_{fuel} is the cost of the fuel, $\eta_{charge-grid}$ is the efficiency of the battery charging from the grid, c_{EE} is the cost from the electric energy taken from the grid, α is the grid emissions factor, WC is the white certificates cost, t is the time and u refers to the control actions.

A list of the penalties (P) considered in this study is reported here:

- Unfeasible motor working points: torques or speeds higher than feasible (P = ∞);
- Unfeasible generator working points: torques or speeds higher than feasible (P = ∞);
- Battery discharging power higher than allowed (P = ∞)
- SOC unfeasible values: if the SOC is higher than 1 or lower than 0.15 (P = ∞)
- $u_1 = 3$ and the power ratio of the ICE is higher than 1 ($\frac{P_{ICE}}{P_e} > 1$) (P = ∞);
- Battery charging power: the maximum charging power is always limited to 2C by the algorithm, but if this limit is reached and $u_1 \neq 0$, then all or part of the ICE power is dissipated and thus a control penalty is added to avoid this condition (P = 100);
- SOC lower than 0.5 and $u_1 = 0$ (P=0.01).

Eq. (16) included an additional term in case the powertrain status (u_1) switched from 0 to any other control in order to consider the fuel needed to turn the ICE on. This has been done by adapting the values reported in [68] to the engine nominal power of the corresponding configuration using a linear approach.

To summarize, the above described procedure allowed to find the control sequence, in terms of powertrain status (u_1) and gear selected (u_2), that minimized the cost function of a powertrain with certain components. The next section deals with the selection of these components.

3.2.2. Components sizing

For optimizing the size of the components of the powertrain the exhaustive search algorithm was used. The components highlighted in green in Fig. 2 were the ones optimized using this methodology, while the size of the components highlighted in blue was defined previous to the optimization procedure. In particular, the electric motor (EM) and inverter (INV) were set to the maximum power that can be delivered by the ICE of the traditional configuration so that both powertrains can perform the same tasks. The transmission system, which includes the Gearbox (GB) and the speed reducer, was designed with two gears possibilities; the first one makes the EM able to provide the maximum torque required during the atomizing and weeding tasks at the corresponding speeds, while the second gear was designed based on the tractor maximum speed. The capacity of the fuel tank was not calculated in this work, but it should be smaller than the one of the conventional configuration, since part of the energy should be provided by the battery. The PTO gear was taken from the conventional configuration.

The exhaust search algorithm can be as explained as follows: a discrete vector of values is provided for the size of each component and all the possible combinations among the different vectors are examined by performing the following steps:

1. Verification of technical feasibility of the components: all the conditions listed below should be verified, otherwise the total cost function for that configuration, $J_{components}$, was set to infinity ($P = \infty$).
   (a) The power of the generator plus two times the battery energy capacity should be higher than the power of the EM (80 kW). This ensures that the newly designed powertrain can deliver the same rated power as the reference tractor, specifically when the battery constantly discharges at a C-rate of 2, which is a reasonably adequate value higher that avoids battery degradation because of extremely fast discharge.
   (b) The sum of the volumes of all the components of the powertrain should be less that the maximum allowable volume. The volume of the components was calculated according to Table 6.
   (c) The power of the generator and ICE should not differ of more than 20%. This flexibility was given in order to consider that the scalable models were not designed to perfectly match with each other.
2. Components scaling: the maximum speed, power and torque of the components were estimated through the scaling procedure reported in [69] represented by the Eqs. (17)–(19). The EM scaling was carried out only one time, since this was the same for all the configurations.

$$x = \sqrt{\frac{P_{scaled}}{P_{base}}} \tag{17}$$

$$\omega_{scaled} = \frac{\omega_{base}}{x} \tag{18}$$

$$\tau_{scaled} = x^2 \tau_{base} \tag{19}$$

3. Control optimization: the procedure described in the previous section was performed using the corresponding components size and their scaled curves. The optimized control cost for the corresponding configuration was obtained.
4. Calculation of the total value of the optimization function: the cost of the powertrain is added to optimized control cost (Eq. (14)). The cost of each component was estimated using the equations reported in Table 6, then the total cost of the hybrid powertrain was calculated assuming that the powertrain represents 30% of the total investment cost. Eq. (20) shows how to estimate the cost of the powertrain, where $Cost_{component}$ corresponds to the cost of the respective component and P to a penalty term, which is calculated based on the conditions reported in point 1.

$$J_{components} = \frac{\sum_{components=0}^{N} Cost_{component}}{0.30} + P \tag{20}$$

The cost fraction reported above has been chosen based on what was reported in [70], from that data it could be estimated that the powertrain share is 40% of the cost of a SUV vehicle. Tractors have more components than on-road vehicles, so the powertrain fraction was assumed to be lower for this type of vehicles.

All the optimization procedure and models described above were implemented using the Open Source Software Python. A simplified scheme of the complete procedure is reported in Fig. 3.

In order to compare the obtained results with the traditional and fully electric configurations, the cost of these powertrains was estimated using the equations of the corresponding components reported in Table 6. Then the total tractor cost was calculated considering that the powertrain represents a 17% and a 50% of the total cost for the traditional and electric vehicles [77], respectively. According to Renius [78], the ICE cost is typically a 19% of the tractor cost, but considering the cost functions of this work and the tractors prices reported in [79] a 14% was found. Therefore, the average between them was taken as reference for this work; this value could vary depending on the function for the ICE price calculation. The fraction of the full electric tractor was defined using what reported in [77]. On the other hand, the operational cost of the traditional configuration was estimated by multiplying the fuel of a cycle (58.31 liters) per the fuel cost and, the number of years and days. Similarly, the one of the electric configuration, even if currently technically unfeasible (Section 3.1.1), was estimated by multiplying the energy required (172.1 kWh) per the electricity cost and its corresponding emissions factors (see the second term of Eq. (15)). Finally, the total cost was estimated as the sum of the control and components contributions.

Finally, to assess the environmental impact of the different solutions, the emissions generated by the systems were calculated. This

Table 6
Functions for the price and volume calculation of the different powertrain components.

Component	Volume m^3	Price [€]	Refs.
ICE	$V_{ICE} = \frac{P_{ICE-d}}{300}$	$Cost_{ICE} = 75 \cdot P_{ICE-d}$	[71]
GEN+REC	$V_{GEN} = \frac{P_{GEN-d}/10 + P_{GEN-d}/13.4}{1000}$	$Cost_{GEN} = 15 \cdot P_{GEN-d} + 200$	[63,72–74]
EM+INV	$V_{EM} = \frac{P_{EM-d}/10 + P_{EM-d}/13.4}{1000}$	$Cost_{EM} = 1.3 \cdot (15 \cdot P_{EM-d} + 200)$	[63,72–74]
BAT	$V_{BAT} = E_{bat}/240$	$Cost_{BAT} = 190 \cdot E_{bat}$	[56,74–76]

All the nominal powers are in kW and the battery energy in kWh.

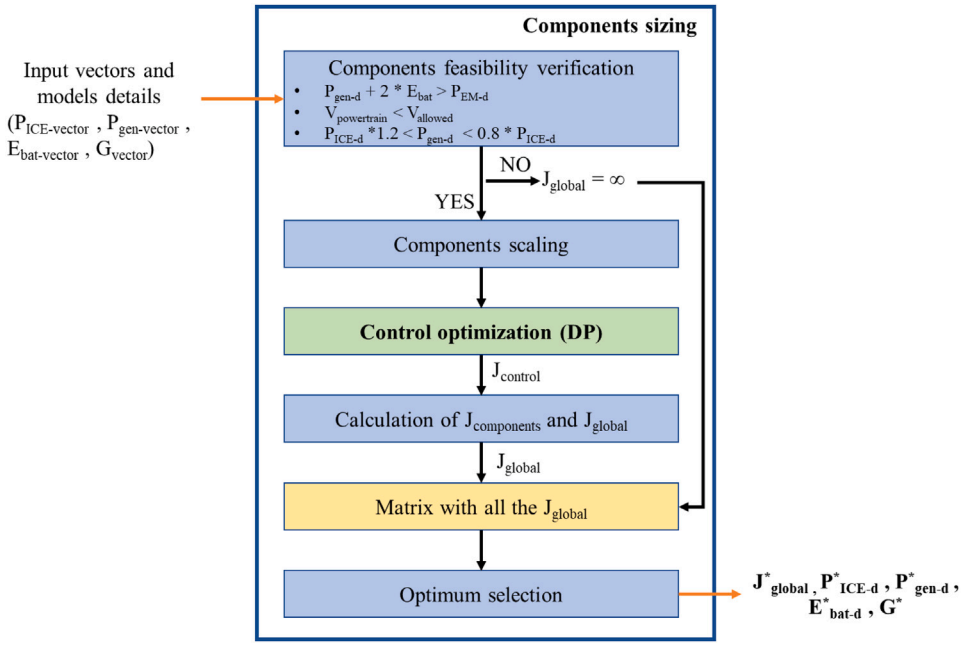

Fig. 3. Optimization procedure scheme.

involved taking into account that every liter of diesel burned results in 2.624 kg of CO_2 emissions. Additionally, the emissions associated with the grid were computed using the grid emission factor denoted as "α". The energy taken from the grid considered its efficiency.

4. Results and analysis

4.1. Input data

The optimization procedure described above was applied to a reference scenario of an European country. The data used for this simulation are shown in Table 7. The ICE and electric machine taken as reference were those pointed in the methodology section. The volume available for the powertrain, the one used to determine whether a configuration was technically feasible, was set to 0.4 m^3; it was defined taking into account the data reported in Table 3 and that additional volume could be obtained from rearranging the components and with a smaller fuel tank. The grid efficiency was set according to [80], while the grid greenhouse emission intensity factor and the white certificates values were taken from [81,82], respectively. Specifically, considering the average value for EU on the years 2020 and 2022, respectively. The drivability coefficients were determined using a simulation-sensitivity approach. The electricity cost, which has strongly fluctuated in the last period and is highly country-dependent, was defined to be 0.26 €/kWh accordingly to the average price in the EU on the first half of 2022 [83]. Diesel is subsidized in many EU countries when used for agricultural purposes. No average value was found for the EU; so, the Italian case was used as reference. In Italy, the average price of agro-diesel on 2021 was 0.87 €/l [84]. This price already considers a tax due to emissions and has strongly varied in recent years, the average price on 2022 was 1.35 €/l, 55% higher than the previous year.

Table 7
Input data.

Variable	Symbol	Value
Volume allowed [m^3]	$V_{allowed}$	0.4
Initial SOC [–]	SOC_o	1
ICE nominal efficiency [–]	η_o	0.38
Reference ICE nominal speed [rpm]	n_{d-ref}	2600
Reference ICE nominal power [kW]	$P_{ICE-d-ref}$	55.4
Reference EM nominal power [kW]	$P_{EM-d-ref}$	80
Reference EM nominal speed [rpm]	$\omega_{EM-d-ref}$	10 000
Reference EM nominal torque [Nm]	$\tau_{EM-d-ref}$	280
Grid efficiency [–]	$\eta_{charge-grid}$	0.86
Grid emissions factor [gCO_2/kWh]	α	265
White certificate cost [€/tonCO_2]	WC	87
Drivability coefficient 1 [€]	β_1	10^{-3}
Drivability coefficient 2 [€]	β_2	10^{-6}
Electricity cost [€/kWh]	c_{EE}	0.26
Agro-diesel cost [€/l]	c_{fuel}	0.87
Gear PTO [–]	–	3.6
GB - gear 0 [–]	–	72[a]
GB - gear 1 [–]	–	167[a]

[a] Total transmission ratio including the Speed Reducer, see Fig. 2.

The input vector that defines the domain of each component to be optimized is reported here:

- Engine nominal power in kW: $P_{ICE-vector} = [30, 40, 50, 55, 60, 70]$;
- Generator nominal power in kW: $P_{gen-vector} = [30, 40, 50, 55, 60, 70]$;

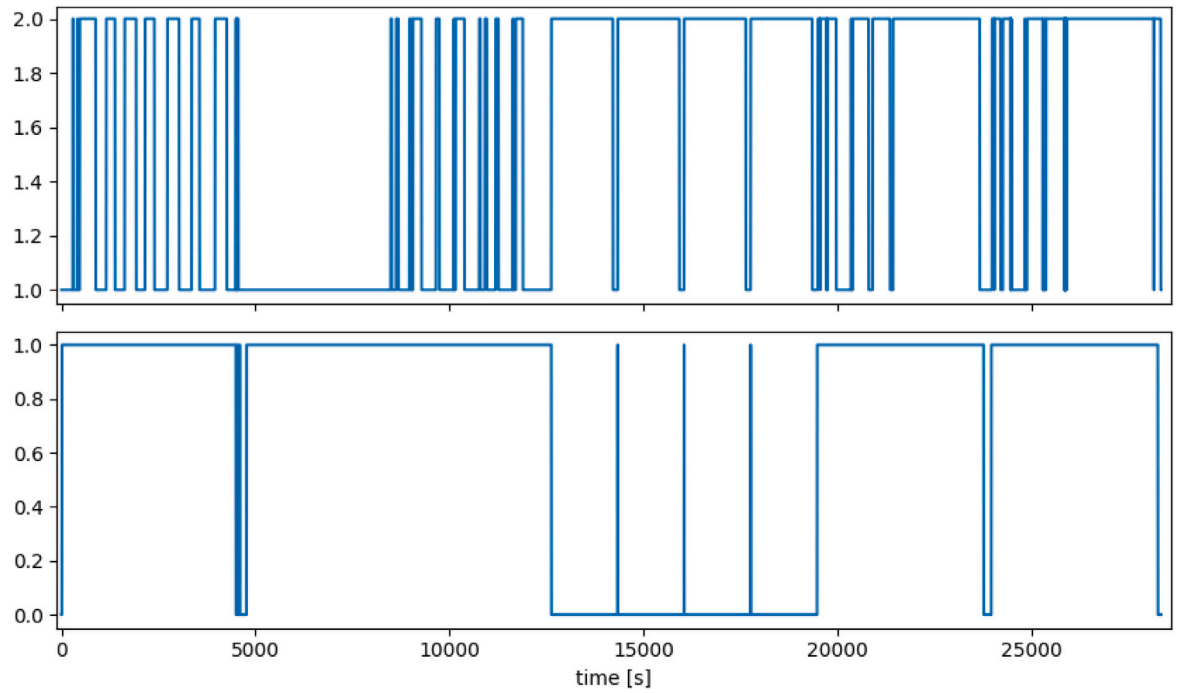

Fig. 4. Optimal control actions: top — powertrain status (u_1) and bottom — selected gear on the transmission system (u_2). Options for the powertrain status: (1) full electric, (2) ICE @ maximum efficiency point, (3) ICE @ maximum power point and (4) All power provided by the ICE.

- Battery energy in kWh: $E_{bat-vector} = [10, 20, 30, 40, 50, 80]$;
- Gear ratio: $G_{vector} = [0.2, 0.25, 0.3]$

4.2. Results — EU generic case

The configuration obtained from the optimization procedure performed with the data reported above is the following: an ICE of 55 kW, a generator of 50 kW, a gear with a transmission ratio of 0.25 between them and a battery with an energy of 20 kWh. The value obtained for the cost function was 96960.92 €. This ICE power enters in the range where the European emissions regulations are less restrictive and therefore, ICEs with simpler emissions control devices could be used. This fact could encourage the manufactures to produce hybrid powertrains. Anyway, the authors believe emissions reduction is crucial and more restrictive standards will also be put in force for small ICEs, but after the technology deployment it would be easier to stay in that path. The total volume of the optimum powertrain is 0.29 m^3. The gearbox is not included, but it is expected to have a limited volume because of its simplicity (2 gears).

The optimal control actions are shown in Fig. 4. In particular, it can be seen that the powertrain status stays all the time between Control 1 — full electric and Control 2 — ICE working at its best efficiency point, which means that the algorithm exploits the advantage of the series architecture. It uses the ICE, which is the critical component in terms of efficiency, only at its maximum efficiency point, either to provide power to the load or to charge the battery. This because the overall efficiency of the system, including the battery to store the energy until it is needed, is higher than the efficiency of the ICE-generator pair when it is forced to work accordingly to the instantaneous power requirements of the load. In other words, the ICE-generator's efficiency when responding to immediate power needs is lower than the efficiency achieved when they operate at their maximum efficiency point together with the battery's charging and discharging efficiency (both processes are needed). This can be explained by the high charging–discharging efficiencies of lithium-ion batteries and the fact that tractors often operate under non-ideal conditions for their powertrain components, resulting in lower efficiency. The latter is due to the bast variety of tasks that a tractor must carry out. This control strategy is reinforced by the drivability coefficients, which make the control to be less variable over time, a feature that can also be favorable for the ICE. The efficiency convenience coupled with the simplicity of series hybrid powertrains may help to explain market preferences. Maximum energy efficiency can be translated into lower fuel consumption and thus less CO_2 emitted, but it is important to note that this relationship is not necessarily linear when considering other types of emissions.

Another aspect that can be noted from Fig. 4 is how the ICE decoupling from the load makes few gear changes necessary during the cycle.

The control strategy can also be seen in Fig. 5, which shows the power distribution among the sources and the battery SOC. The black curve shows the output power of the EM so the one required by the traction and PTO. Similarly, the other curves show the output power at the corresponding components; unless the yellow curve, marked as P_{inv} that shows the input power at the inverter. In other words, the difference between the black and yellow curves is due to the efficiency of the EM and the inverter. Fig. 5 — left shows how full electric mode ($u_1 = 0$) is mainly used when the power required is considerably low as for tying and also at the beginning of the cycle when the SOC is so high that could limit the use of the ICE at its maximum efficiency point. In the last half of the cycle, it could be clearly noticed how the battery is used to boost the action of the GENSET group.

The efficiency map of the EM with the working points is reported in Fig. 6-left. The working points while atomizing can be identified because of the fixed speed in this working condition. In the same way, most of the points in the high speed region could be related to transportation. Although, the wide difference among the working points of the EM, the efficiency of the EM and inverter combined is most of the time above 0.81 and the lowest efficiency registered was of 0.745 (see Fig. 6-right). The average efficiency of the EM during the cycle was 0.87, while the average of the simplified efficiency of this powertrain calculated as the multiplication of the efficiency of the EM, ICE and generator was 0.32, when the battery efficiency is considered this efficiency lowered to 0.30, which is higher than the typical average efficiency of a conventional powertrain during a complete cycle. This

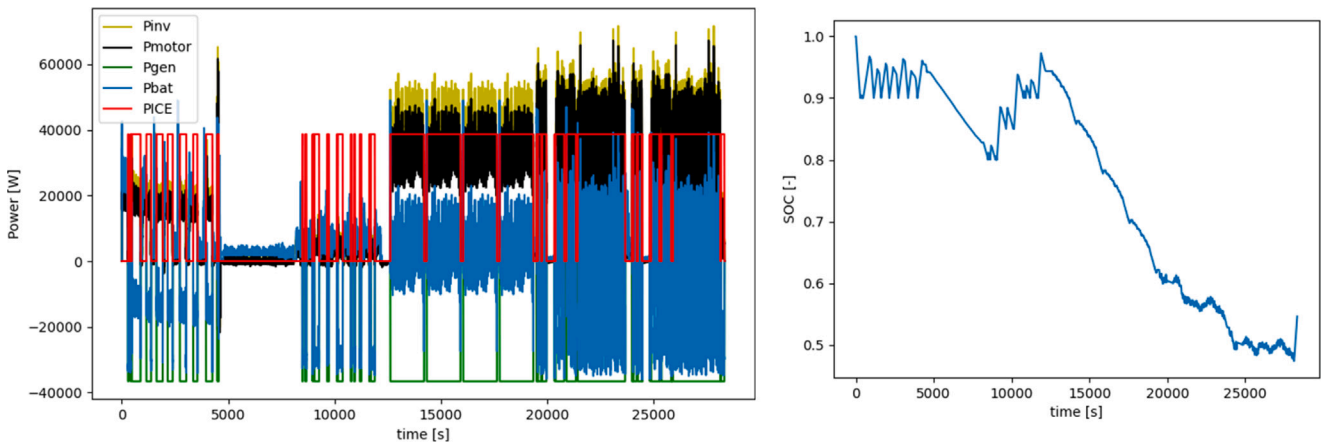

Fig. 5. Power distribution (left) and SOC (right) during the 8 h duty cycle considered.

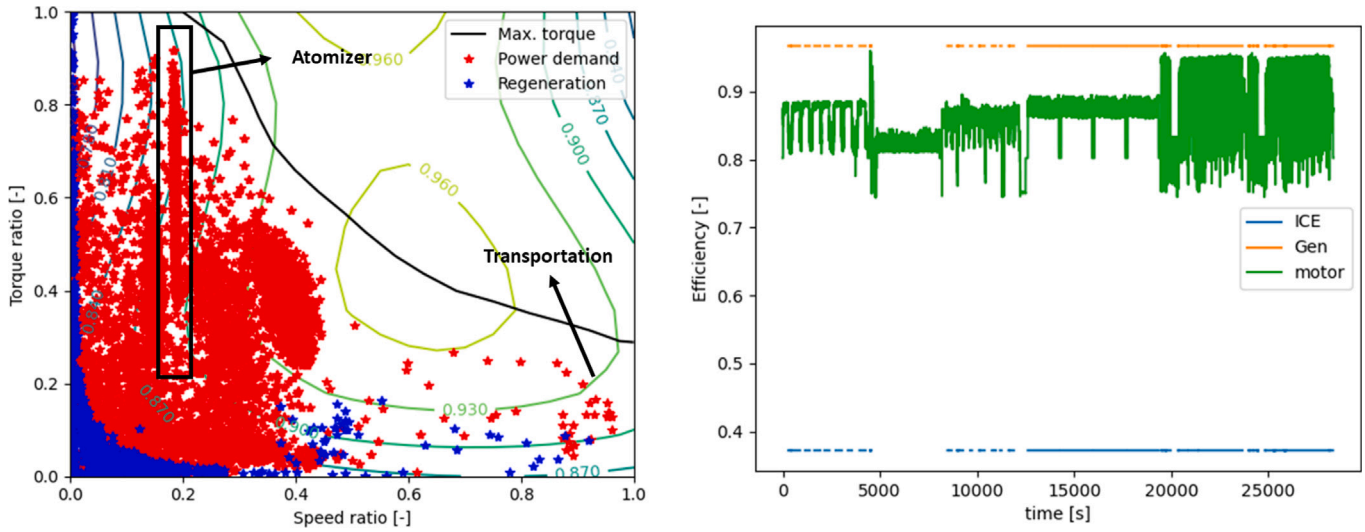

Fig. 6. EM efficiency map (left) and cycle efficiency curves (right).

demonstrates the potential of series hybrid powertrains to improve efficiency and fuel consumption, more detailed comparisons are provided in what follows.

The ICE and generator efficiencies were 0.37 and 0.97, when working at its maximum efficiency point. The efficiency map of these machines with the corresponding working point is reported in Fig. 7. It could be seen how the optimization procedure selected components that almost perfectly match their maximum efficiency points, this includes the gear ratio between the ICE and the generator.

From the obtained value for the cost function (96960.92 €) 37% corresponds to the fixed cost and 63% to the operational cost. It should be highlighted that this cost includes the emissions costs; if this was not the case, the total value will be lower. On the other hand, maintenance costs were not considered in this work; if that were the case a greater contribution from the operational costs should be expected. The cost function value for the traditional and electric configuration was 106315.0 €and 164639.0 €, respectively; so the hybrid solution is the most convenient. For the electric configuration, the components costs represent a large fraction of the total due to the price of the battery. The convenience of this type of configuration usually increases when the maintenance costs are taken into account, the opposite occurs for the traditional configuration.

The greenhouse emissions, due to the tractor operation, are reduced when a hybrid configuration is used. It was calculated that the tractor in this study generates 170.61 tons of CO_2 in operation over its lifetime, which is 20% less than the traditional architecture. The latter generates 214.20 tons of CO_2. The electric configuration, which is not yet viable, would only produce 74.24 tons of CO_2, assuming the average emission factor for the EU reported above. This does not consider the emissions produced to build the components.

4.3. Sensitivity analysis

The input parameters considered in this work have values that change depending on the country, technological advancements, worldwide situation and period of time. In addition, accurate values of some of these parameters are difficult to find and manufacturers should consider the situation in different countries and with different scenarios to decide their investments. All this makes a sensitivity analysis important to understand the convenience of series hybrid powertrains for tractors. The parameters studied in this work were: (i) fuel cost; (ii) electricity price; (iii) grid emission factor; (iv) White Certificates cost and (v) battery price. The price of the fuel was considered to vary from 0.2 €/l to 2.2 €/l according to [84–86], this price have oscillated in Spain between 0.68 €/l and 0.95 €/l in the period 2019–2021, in Italy between 0.62 €/l and 1.52 €/l in the period 2015–2022 and it is currently (Dec, 2022) around 1.6 €/l in Germany. In the latter, the farmers buy diesel at the market price, but they can apply for a tax relief of about 0.21 €/l [86]. A similar approach is used in Sweden where diesel's price is even higher. In this study, the electricity cost ranged from

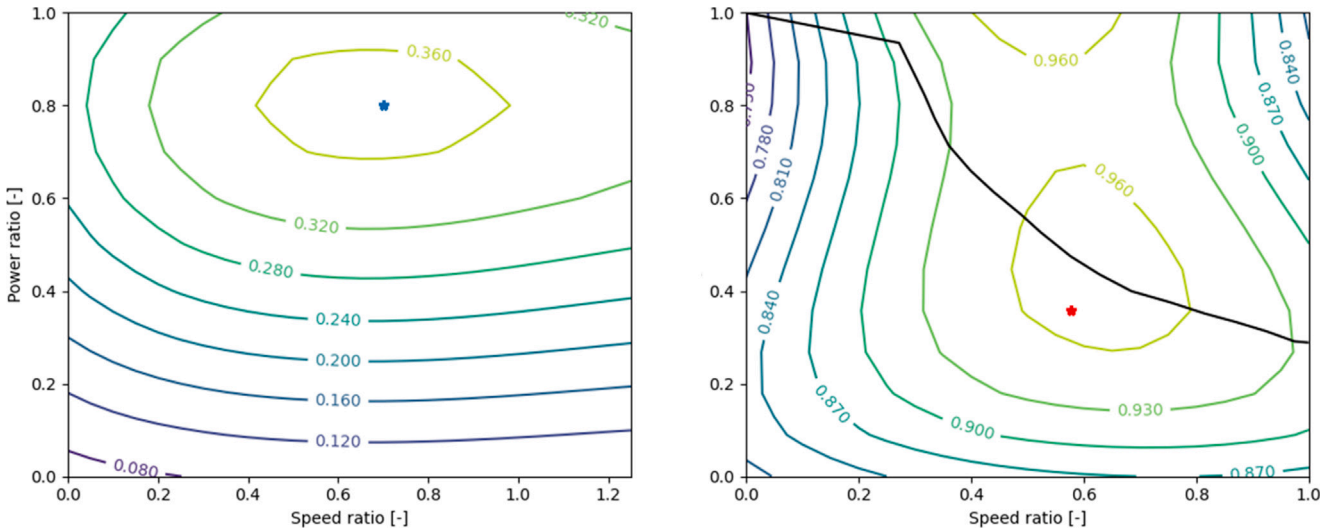

Fig. 7. Efficiency maps: left-ICE and right-generator.

0 €/kWh, when the energy is self-produced, to 0.6 €/kWh. This range was selected based on what reported in [83] for different European countries. Similarly, the range studied for the grid emission factor, White Certificate cost and battery price considered was 0–500, 0–150 and 50–250, respectively. Fig. 8 shows the results of this analysis. At this step each parameter is studied separately; thus, the others maintain their reference value. The parameters that have a higher impact on the global optimization function are: fuel cost, battery price and electricity cost. In the case of the cost of fuel, the cost function increased by 99% when the cost of fuel increased by 153% and instead had a reduction of 43% when the price was 77% lower. On the other hand, grid emission factor and White Certificates cost had a very limited impact, below 2%; due of this, the White Certificate cost curve is not reported.

Fig. 8 also reports a comparison with the traditional and electrical architectures. The sensitivity analysis in terms of fuel shows that the traditional architecture is the most convenient when the fuel price is below 0.6 €/l, while the electric configuration is the preferred one when the fuel price is almost 1.8 €/l and it becomes better than the traditional one when the fuel cost is more than 1.6 €/l. The variation of the electricity price has a higher impact on the electric configuration and a limited one on the hybrid configuration. The convenience of the latter compared to the traditional architecture reduces when the electricity price increases. The full electric architecture is the more profitable in case of self-produced energy, which could be a feasible scenario during summer. The fact that the optimization function has a higher value when the electricity price is 0.1 €/kWh is due to bad decisions in the control policy when the SOC was higher than 0.9. In other words, the battery was discharged too fast at the beginning of the cycle, causing it to not have enough energy for the remaining part, but as this occurred when the SOC was higher than 0.9, the algorithm was not able to backtrack before this decision or set of decisions were taken. This impact the total final cost. If the same policy of the next point (0.2 €/kWh) was used, the value of the optimization function is expected to be lower or equal to that of the next point. This could also be avoided with a fitter discretization of the state variable (SOC).

The variations of the grid emissions intensity factor do not produce changes in which is the best type of configuration and have a higher impact on the global cost function of the electric configuration. Lastly, the hybrid configuration is the most convenient architecture within the complete range of battery prices considered. Battery price has an important effect on the global cost function of the electric configuration, making it more convenient than the traditional one when the battery price is below 80 €/kWh. Decreasing battery prices narrows the gap between the hybrid and electric configuration, suggesting that this trend combined with the variation of another variable could make the electric configuration the most suitable in the future. Anyway, with the energy density of batteries at the moment, a full electric configuration is not technically feasible as discussed in the previous sections.

Since the operational costs represent the largest fraction of the total and fuel and electricity prices are its main parameters, a further analysis considering the variation of these two factors simultaneously has been carried out. Moreover, these two parameters vary considerably among the different countries and period of the year. Fig. 9-left shows that the hybrid configuration is the most favorable in most of the cases. In addition, it shows the best type of configuration for different scenarios created considering the conditions in December 2022 in different countries. In particular, a hybrid configuration with a small battery is the most convenient for the countries in the "south" of Europe and the UK where agrodiesel has relatively moderate prices, while a hybrid configuration with a battery bigger than 20 kWh is the most convenient in countries like Sweden. The reduction of battery prices, which is expected, will further favor the use of hybrid powertrains and increase battery sizes. In other words, in the future it would be expected to have more dark blue dots in Fig. 9-left.

Fig. 9-right shows what would happen if the energy density of batteries were to increase to the point where electric configurations with an autonomy greater than 8 h were technically feasible. In that case, the full electric configuration will be convenient when electricity price is low (or self-production) and diesel price is high. In fact, due to the efforts of the authorities to achieve the reduction of greenhouse emissions by 2050, it is expected that the taxes for fuels will increase in the coming years. It could be noted that the transition on when an electric or a hybrid configuration is convenient bypasses the "big" battery hybrids. This fact could be explained by the following reasons: (i) the small hybrids have a battery with enough energy to make the ICE always work with high efficiency; a slightly bigger battery would only require a higher investment, but without the capacity to provide all the energy; therefore, the tractor will continue to depend on the ICE; (ii) the cost fraction of the powertrain with respect to the total tractor cost was assumed constant, but bigger batteries would represent a higher percentage of the total cost.

Finally, the impact of the fuel and battery price was studied together, Fig. 10 shows the results of this study. Also in this case the hybrid configuration is the most convenient in most of the scenarios. The orange rectangle highlights the region corresponding to current battery prices, the traditional configuration is not more convenient when the fuel costs more than 0.6 €/l. On the other hand, bigger batteries are desirable when the battery price decreases below 175 €/kWh

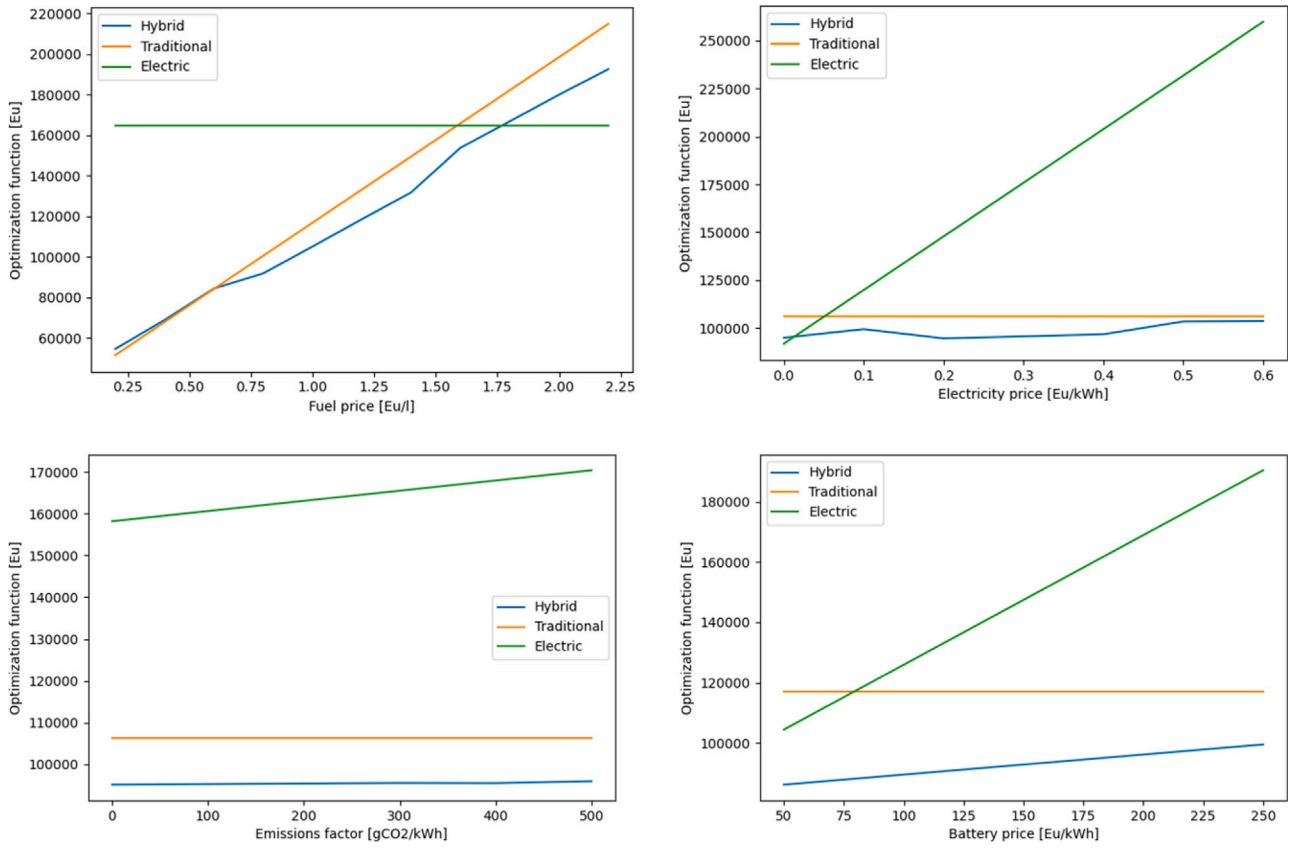

Fig. 8. Sensitivity analysis results — 1st row: fuel and electricity prices; — 2nd row: Emissions intensity factor and Battery price.

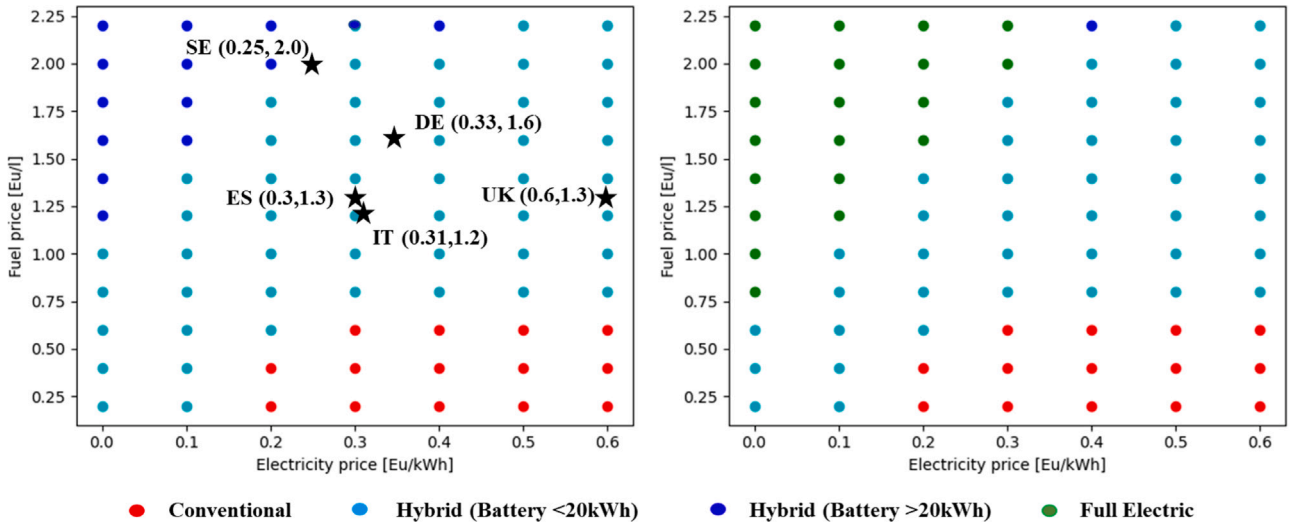

Fig. 9. Best typology of powertrain configuration considering fuel and electricity price. Left — current battery energy density, right — battery with double energy density.

and the one of fuel increases above 1.5 €/l. Similarly to what reported before, Fig. 10-right presents the scenario with an increase in the battery energy density. Electric tractors would be convenient in case of low battery prices and high fuel prices.

The condition reported in Figs. 9-right and 10-right could also be accomplished with improvements in the density of the other powertrain components and a rearranging of the tractor architecture, but this is an unlikely situation.

Summing up, the future of series powertrains seems to be promising for agricultural machinery, but also already convenient with the current scenarios. More detailed comparisons with the parallel configuration are needed to understand if this configuration could bring further benefits.

5. Conclusions

Hybrid powertrains with a series configuration for tractors has not been deeply studied by the academia, while they have received considerable attention at an industrial level. In addition, a detailed investigation of the optimal sizing of the powertrain components has not been carried out considering real data, realistic control strategy and design constraints. In this work, a series hybrid powertrain model was

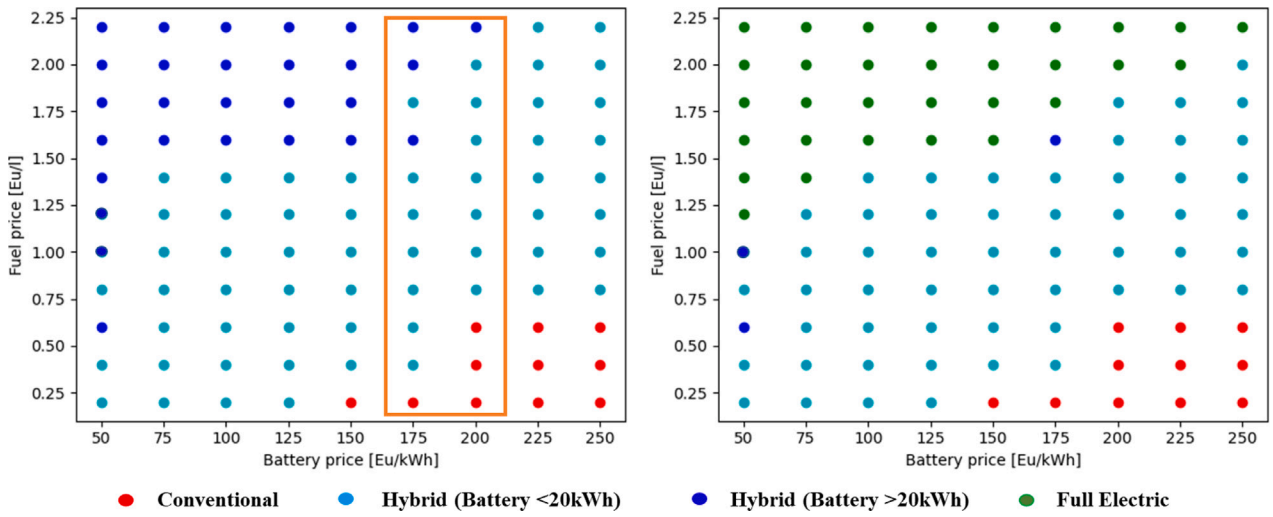

Fig. 10. Best typology of powertrain configuration considering fuel and battery price. Left — current battery energy density, right — battery with double energy density.

built, then its control and components size were optimized for a vineyard/orchard tractor using real field data. The optimization procedure implemented is two-level and based on DP. The optimization function introduced considers both environmental and economical aspects. Volume was demonstrated to play a key role in the design of powertrains for tractors; thus, a space constraint was introduced. The results showed how the optimization procedure exploited the disconnection between the load and the ICE to maximize the powertrain efficiency, making it higher than the average efficiency of a powertrain with the traditional configuration. In a generic European scenario, the optimal powertrain has an ICE with an optimal power below 56 kW, where the emissions regulations are less restrictive. In addition, the sensitivity analysis carried out shows that hybrid powertrains have enormous potential in the agricultural market; since it is the most convenient type of architecture for the scenarios studied for different European countries and with the upcoming emissions standards and fuel increasing prices through taxes this trend will intensify. Moreover, the battery price reduction could also contribute to this trend. The threshold values of battery price, fuel cost and electricity costs at which the transition to hybrid or electric tractor is convenient are assessed.

As further work, the authors consider that it would be interesting to study the impact of the maintenance costs on the conclusions drawn in this study. Theoretically, they should favor the electric configuration, but the possible substitution of the battery could play a key role; this latter issue is the most expensive component of the powertrain. Moreover, a detailed comparison with the parallel powertrain configuration is suggested, although this apparently goes in a different direction than the current interests of the industry.

CRediT authorship contribution statement

Manuel Antonio Perez Estevez: Writing – review & editing, Writing – original draft, Software, Methodology, Investigation, Formal analysis, Data curation, Conceptualization. **Joaquim Melendez Frigola:** Writing – review & editing, Validation, Supervision, Methodology, Conceptualization. **Joaquim Armengol Llobet:** Writing – review & editing, Supervision, Methodology, Formal analysis, Conceptualization. **Luigi Alberti:** Writing – review & editing, Funding acquisition, Conceptualization. **Massimiliano Renzi:** Writing – review & editing, Supervision, Methodology, Investigation, Formal analysis, Conceptualization.

Declaration of competing interest

The authors declare the following financial interests/personal relationships which may be considered as potential competing interests: Luigi Alberti reports financial support was provided by Italian Ministry for University and Research. Luigi Alberti reports a relationship with Italian Ministry for University and Research that includes: funding grants.

Acknowledgment

This work was supported by the Project “Green SEED: Design of more-electric tractors for a more sustainable agriculture” funded by the Italian Ministry for University and Research under PRIN 2017 call, grant n. 2017SW5MRC - CUP I54I18000340001.

Data availability

The authors do not have permission to share data.

References

[1] Janulevičius A, Juostas A, Čiplienė A. Nitrogen-oxide emissions from diesel-engine farm tractors during real-life cycles and their correlation with the not-to-exceed operating zones. Biosyst Eng 2017;161:93–105.
[2] United Nations - Climate Change. The Paris Agreement. 2022, Consulted December, https://unfccc.int/process-and-meetings/the-paris-agreement/the-paris-agreement.
[3] Lovarelli D, Bacenetti J. Exhaust gases emissions from agricultural tractors: State of the art and future perspectives for machinery operators. Biosyst Eng 2019;186:204–13.
[4] McCormick Power Technology. Stage V: new challenges to reduce tractor emissions. 2020, https://www.mccormick.it/as/stage-v-new-challenges-to-reduce-tractor-emissions/.
[5] García A, Monsalve-Serrano J, Martínez-Boggio S, Wittek K. Potential of hybrid powertrains in a variable compression ratio downsized turbocharged VVA spark ignition engine. Energy 2020;195:117039.
[6] Millo F, Cubito C, Rolando L, Pautasso E, Servetto E. Design and development of an hybrid light commercial vehicle. Energy 2017;136:90–9.
[7] USDepartment of Energy. Electric vehicle benefits and considerations. 2022, Consulted December, URL https://afdc.energy.gov/fuels/electricity_benefits.html.
[8] Murgovski N, Hu X, Johannesson L, Egardt B. Combined design and control optimization of hybrid vehicles. 2015.
[9] Hu X, Han J, Tang X, Lin X. Powertrain design and control in electrified vehicles: A critical review. IEEE Trans Transp Electrif 2021;7(3):1990–2009.
[10] Sorrentino M, Cirillo V, Nappi L. Development of flexible procedures for co-optimizing design and control of fuel cell hybrid vehicles. Energy Convers Manage 2019;185:537–51.
[11] Brenna M, Foiadelli F, Leone C, Longo M, Zaninelli D. Feasibility proposal for heavy duty farm tractor. In: 2018 International conference of electrical and electronic technologies for automotive. IEEE; 2018, p. 1–6.
[12] Chen Y, Xie B, Du Y, Mao E. Powertrain parameter matching and optimal design of dual-motor driven electric tractor. Int J Agric Biol Eng 2019;12(1):33–41.

[13] McCormick Power Technology. The tractor of the future: connectivity and electrification. 2022, https://www.mccormick.it/as/the-tractor-of-the-future-connectivity-and-electrification/.

[14] European Agriculture Machinery Association. Engine emissions – stage V. 2018, https://www.cema-agri.org/environmental-protection-article-right.

[15] Mocera F, Martini V, Somà A. Comparative analysis of hybrid electric architectures for specialized agricultural tractors. Energies 2022;15(5):1944.

[16] Lagnelöv O, Dhillon S, Larsson G, Nilsson D, Larsolle A, Hansson P-A. Cost analysis of autonomous battery electric field tractors in agriculture. Biosyst Eng 2021;204:358–76.

[17] Deere J. Future of farming. 2022, Consulted December, https://www.deere.co.uk/en/agriculture/future-of-farming/.

[18] Erkelens JV. VIDEO | john deere shows autonomous electric tractor. 2022, Consulted December, https://www.futurefarming.com/tech-in-focus/autonomous-semi-autosteering-systems/video-john-deere-shows-autonomous-electric-tractor/.

[19] Bin X, Hao L, Zheng-He S, En-Rong M. Powertrain system design of medium-sized hybrid electric tractor. Inform Technol J 2013;12(23):7228.

[20] Dalboni M, Santarelli P, Patroncini P, Soldati A, Concari C, Lusignani D. Electrification of a compact agricultural tractor: A successful case study. In: 2019 IEEE transportation electrification conference and expo. IEEE; 2019, p. 1–6.

[21] International Council on Clean Transportation. European stage V non-road emission standars. Policy update 2016.

[22] Beligoj M, Scolaro E, Alberti L, Renzi M, Mattetti M. Feasibility evaluation of hybrid electric agricultural tractors based on life cycle cost analysis. IEEE Access 2022;10:28853–67.

[23] Mocera F. A model-based design approach for a parallel hybrid electric tractor energy management strategy using hardware in the loop technique. Vehicles 2020;3(1):1–19.

[24] Troncon D, Alberti L, Mattetti M. A feasibility study for agriculture tractors electrification: Duty cycles simulation and consumption comparison. In: 2019 IEEE transportation electrification conference and expo. IEEE; 2019, p. 1–6.

[25] Liu Z, Onori S, et al. Simultaneous design and control optimization of a series hybrid military truck. Tech. rep., SAE Technical Paper; 2018.

[26] Nakka SKS, Alexander-Ramos MJ. Simultaneous combined optimal design and control formulation for aircraft hybrid-electric propulsion systems. J Aircr 2021;58(1):53–62.

[27] Makaras R, Lukoševičius V, Keršys A, et al. Evaluation of the working parameters of a series-hybrid tractor under the soil work conditions. Tehn vjesnik 2022;29(1):45–50.

[28] Jia C, Qiao W, Qu L. Modeling and control of hybrid electric vehicles: a case study for agricultural tractors. In: 2018 IEEE vehicle power and propulsion conference. IEEE; 2018, p. 1–6.

[29] Jia C, Qiao W, Qu L. Numerical methods for optimal control of hybrid electric agricultural tractors. In: 2019 IEEE transportation electrification conference and expo. IEEE; 2019, p. 1–6.

[30] Kubota Corporation. Compact electric tractor LXe-261 released in European markets. 2022, https://www.kubota.com/news/2022/20220905.html.

[31] Monarch Tractor. Working toward a future with clean farming. 2022, Consulted December, https://www.monarchtractor.com/homepage.

[32] Fendt. Fendt future farm -fendt e100 vario. Nuestro acceso al futuro.. 2022, Consulted December, https://www.fendt.com/es/e100-vario.

[33] Solectrac. Solectrac-homepage. 2022, Consulted December, https://solectrac.com/about.

[34] Hattum BV. John deere releases video of gridcon electric tractor. 2022, Consulted December, https://www.futurefarming.com/tech-in-focus/john-deere-releases-video-of-gridcon-electric-tractor/.

[35] Mocera F, Somà A. Analysis of a parallel hybrid electric tractor for agricultural applications. Energies 2020;13(12):3055.

[36] Troncon D, Alberti L. Case of study of the electrification of a tractor: Electric motor performance requirements and design. Energies 2020;13(9):2197.

[37] KannusamyMY L, Ravindran V, Rao N. Analysis of multiple hybrid electric concept in agricultural tractor through simulation technique. Tech. rep, SAE Technical Paper; 2019.

[38] Lee D-H, Kim Y-J, Choi C-H, Chung S-O, Inoue E, Okayasu T. Development of a parallel hybrid system for agricultural tractors. 2017.

[39] Troncon D, Alberti L, Bolognani S, Bettella F, Gatto A. Electrification of agricultural machinery: A feasibility evaluation. In: 2019 Fourteenth international conference on ecological vehicles and renewable energies. IEEE; 2019, p. 1–7.

[40] Kim YJ, Song B, Kim J. Load torque estimation for a parallel hybrid agricultural tractor in field operations. Int J Precis Eng Manuf 2013;14(10):1865–8.

[41] Barthel J, Gorges D, Bell M, Munch P. Energy management for hybrid electric tractors combining load point shifting, regeneration and boost. In: 2014 IEEE vehicle power and propulsion conference. IEEE; 2014, p. 1–6.

[42] Ghobadpour A, Mousazadeh H, Kelouwani S, Zioui N, Kandidayeni M, Boulon L. An intelligent energy management strategy for an off-road plug-in hybrid electric tractor based on farm operation recognition. IET Electr Syst Transp 2021;11(4):333–47.

[43] Zhu Z, Lai L, Sun X, Chen L, Cai Y. Design and analysis of a novel mechanic-electronic-hydraulic powertrain system for agriculture tractors. IEEE Access 2021;9:153811–23.

[44] Dou H, Wei H, Zhang Y, Ai Q. Configuration design and optimal energy management for coupled-split powertrain tractor. Machines 2022;10(12):1175.

[45] Steyr. Steyr hybrid drivetrain konzept top-efficiency ahead. 2022, Consulted December, https://www.steyr-traktoren.com/en-distributor/agriculture/technologie/steyr-hybrid-drivetrain-konzept.

[46] Agrario EC. SRX hybrid (102 HP): nace el concepto de la tecnología achybrid. 2022, Consulted December, https://ecomercioagrario.com/srx-hybrid-102-hp-nace-el-concepto-de-la-tecnologia-achybrid/.

[47] Deere J. 944K hybrid wheel loader. 2022, Consulted December, https://www.deere.com/en/loaders/wheel-loaders/large-wheel-loaders/944k-wheel-loader/.

[48] Ishida K, Higurashi M. Hybrid wheel loaders incorporating power electronics. Hitachi Rev 2015;64(7):398–402.

[49] Yamazaki Y, Saiki S, Koga N, Tsutsui A, Sekiyama K, Maeda K. Development of 20-tonne class hybrid excavator, SK200h-10. 2019.

[50] Forsttechnik K. K 507E-H. 2022, Consulted December, https://www.kollergmbh.com/en/yarder/k507/k-507e-h.

[51] Leitalpin. Mainpage - we strive to make you more profitable. 2022, Consulted December, https://www.leitalpin.com/en/.

[52] Lajunen A, Kivekäs K, Freyermuth V, Vijayagopal R, Kim N. Simulation-based assessment of energy consumption of alternative powertrains in agricultural tractors. World Electr Veh J 2024;15(3):86.

[53] Pascuzzi S, Łyp-Wrońska K, Gdowska K, Paciolla F. Sustainability evaluation of hybrid agriculture-tractor powertrains. Sustainability 2024;16(3):1184.

[54] Diesel Net. Emission test cycles - nonroad transient cycle (NRTC). 2022, Consulted December, https://dieselnet.com/standards/cycles/nrtc.php.

[55] Pierri E, Cirillo V, Vietor T, Sorrentino M. Adopting a conversion design approach to maximize the energy density of battery packs in electric vehicles. Energies 2021;14(7):1939.

[56] Zeng X, Li M, Abd El-Hady D, Alshitari W, Al-Bogami AS, Lu J, et al. Commercialization of lithium battery technologies for electric vehicles. Adv Energy Mater 2019;9(27):1900161.

[57] Kwao-Boateng E, Ankudey EG, Darkwah L, Danquah KO. Assessment of diesel fuel quality. Heliyon 2024;10(2).

[58] Scolaro E, Beligoj M, Estevez MP, Alberti L, Renzi M, Mattetti M. Electrification of agricultural machinery a review. IEEE Access 2021.

[59] Ben-Chaim M, Shmerling E, Kuperman A. Analytic modeling of vehicle fuel consumption. Energies 2013;6(1):117–27.

[60] Vukovic M, Leifeld R, Murrenhoff H. Reducing fuel consumption in hydraulic excavators—A comprehensive analysis. Energies 2017;10(5):687.

[61] Hansson P, Lindgren M, Nordin M, Pettersson O. A methodology for measuring the effects of transient loads on the fuel efficiency of agricultural tractors. Appl Eng Agric 2003;19(3):251.

[62] Lindgren M, Hansson P-A. Effects of transient conditions on exhaust emissions from two non-road diesel engines. Biosyst Eng 2004;87(1):57–66.

[63] Burress T. Benchmarking state-of-the-art technologies. In: Oak ridge national laboratory (ORNL), 2013 US DOE hydrogen and fuel cells program and vehicle technologies program annual merit review and peer evaluation meeting. 2013.

[64] Li K, Tseng KJ. Energy efficiency of lithium-ion battery used as energy storage devices in micro-grid. In: IECON 2015-41st annual conference of the IEEE industrial electronics society. IEEE; 2015, p. 005235–40.

[65] Bacenetti J. How does annual utilisation can affect the environmental impact of tractors? A life-cycle assessment comparing hypothetical scenarios for farmers and agricultural contractors in northern Italy. Biosyst Eng 2022;213:63–75.

[66] Roberts SM. Dynamic programming in chemical engineering and process control by Sanford M Roberts. Elsevier; 1964.

[67] Cooper L, Cooper MW. Introduction to dynamic programming: International series in modern applied mathematics and computer science, volume 1, vol. 1, Elsevier; 2016.

[68] Varani M, Estevez MAP, Renzi M, Alberti L, Mattetti M. Controlling idling: a ready-made solution for reducing exhaust emissions from agricultural tractors. Biosyst Eng 2022;221:283–92.

[69] Ivanco A, Filipi Z. Framework for powerpack optimization in the SHEV: two stage optimization for best efficiency in the hybrid electric vehicle powertrain design. In: 2015 IEEE vehicle power and propulsion conference. IEEE; 2015, p. 1–4.

[70] Lutsey N, Nicholas M. Update on electric vehicle costs in the United States through 2030. Int Counc Clean Transp 2019;12.

[71] Kleiner F, Friedrich HE. Development of a transport application based cost model for the assessment of future commercial vehicle concepts. 2017.

[72] Delucchi MA, Lipman TE. Lifetime cost of battery, fuel-cell, and plug-in hybrid electric vehicles. Electr Hybrid Veh Power Sour Models, Sustain Infrastruct Market. Amsterdam, the Netherlands 2010;19–60.

[73] Schröter J. Development of high speed electrical drives for mobile machinery: Challenges and potential solutions. 2015.

[74] Wen J, Zhao D, Zhang C. An overview of electricity powered vehicles: Lithium-ion battery energy storage density and energy conversion efficiency. Renew Energy 2020;162:1629–48.

[75] Muralidharan N, Self EC, Nanda J, Belharouak I. Next-generation cobalt-free cathodes–a prospective solution to the battery industry's cobalt problem. Transit Metal Oxides Electrochem Energy Storage 2022;33–53.

[76] Deng D. Li-ion batteries: basics, progress, and challenges. Energy Sci Eng 2015;3(5):385–418.
[77] Ruffo GH. How much does the powertrain represent out of total cost for an EV? INSIDEEVs 2020.
[78] Renius KT. Fundamentals of tractor design. Springer; 2020.
[79] Spinelli R, Magagnotti N, Nati C. Harvesting vineyard pruning residues for energy use. Biosyst Eng 2010;105(3):316–22.
[80] Sears J, Roberts D, Glitman K. A comparison of electric vehicle level 1 and level 2 charging efficiency. In: 2014 IEEE conference on technologies for sustainability (susTech). IEEE; 2014, p. 255–8.
[81] European Environment Agency. Greenhouse gas emission intensity of electricity generation in Europe. 2022, https://www.eea.europa.eu/ims/greenhouse-gas-emission-intensity-of-1.
[82] Tiseo I. Prices of carbon trading worldwide 2022, by jurisdiction. 2022, https://www.statista.com/statistics/1241719/carbon-trading-prices-worldwide-by-select-country/.
[83] Eurostat. Electricity price statistics. 2022, https://ec.europa.eu/eurostat/statistics-explained/index.php?title=Electricity_price_statistics.
[84] TESEO. Milan: Agricultural diesel price. 2022, https://teseo.clal.it/en/?section=gasolio_agricolo.
[85] Lucia F. Monthly price of marine and agricultural diesel per liter in Spain 2019–2021. 2022, https://www.statista.com/statistics/1197413/monthly-price-marine-and-agricultural-diesel-per-liter-spain/.
[86] Brandenburg A. Landwirte fordern aussetzung der besteuerung für agrardiesel. 2022, https://www.rbb24.de/studiofrankfurt/wirtschaft/2022/06/diesel-preise-landwirte-steuer-aussetzung.html.